



The Usage of Parameterized Fatigue Spectra and Physics-Based Systems Engineering Models for Wind Turbine Component Sizing

Preprint

Taylor Parsons, Yi Guo, Paul Veers,
Katherine Dykes, and Rick Damiani
National Renewable Energy Laboratory

*Presented at the American Institute of Aeronautics and
Astronautics Science and Technology Forum and Exposition
(SciTech 2016)
San Diego, California
January 4–8, 2016*

**NREL is a national laboratory of the U.S. Department of Energy
Office of Energy Efficiency & Renewable Energy
Operated by the Alliance for Sustainable Energy, LLC**

This report is available at no cost from the National Renewable Energy Laboratory (NREL) at www.nrel.gov/publications.

Conference Paper
NREL/CP-5000-65515
January 2016

Contract No. DE-AC36-08GO28308

NOTICE

The submitted manuscript has been offered by an employee of the Alliance for Sustainable Energy, LLC (Alliance), a contractor of the US Government under Contract No. DE-AC36-08GO28308. Accordingly, the US Government and Alliance retain a nonexclusive royalty-free license to publish or reproduce the published form of this contribution, or allow others to do so, for US Government purposes.

This report was prepared as an account of work sponsored by an agency of the United States government. Neither the United States government nor any agency thereof, nor any of their employees, makes any warranty, express or implied, or assumes any legal liability or responsibility for the accuracy, completeness, or usefulness of any information, apparatus, product, or process disclosed, or represents that its use would not infringe privately owned rights. Reference herein to any specific commercial product, process, or service by trade name, trademark, manufacturer, or otherwise does not necessarily constitute or imply its endorsement, recommendation, or favoring by the United States government or any agency thereof. The views and opinions of authors expressed herein do not necessarily state or reflect those of the United States government or any agency thereof.

This report is available at no cost from the National Renewable Energy Laboratory (NREL) at www.nrel.gov/publications.

Available electronically at SciTech Connect <http://www.osti.gov/scitech>

Available for a processing fee to U.S. Department of Energy and its contractors, in paper, from:

U.S. Department of Energy
Office of Scientific and Technical Information
P.O. Box 62
Oak Ridge, TN 37831-0062
OSTI <http://www.osti.gov>
Phone: 865.576.8401
Fax: 865.576.5728
Email: reports@osti.gov

Available for sale to the public, in paper, from:

U.S. Department of Commerce
National Technical Information Service
5301 Shawnee Road
Alexandria, VA 22312
NTIS <http://www.ntis.gov>
Phone: 800.553.6847 or 703.605.6000
Fax: 703.605.6900
Email: orders@ntis.gov

Cover Photos by Dennis Schroeder: (left to right) NREL 26173, NREL 18302, NREL 19758, NREL 29642, NREL 19795.

NREL prints on paper that contains recycled content.

Using Parameterized Fatigue Spectra and Physics-Based Systems Engineering Models to Size Wind Turbine Components*

Taylor J. Parsons[†], Yi Guo[‡], Paul Veers[§], Katherine Dykes[¶] and Rick Damiani^{||}
National Renewable Energy Laboratory, Golden, CO, 80401.

Software models that use design-level input variables and physics-based engineering analysis for estimating the mass and geometrical properties of components in large-scale machinery can be very useful for analyzing design trade-offs in complex systems. This study uses DriveSE, an OpenMDAO-based drivetrain model that uses stress and deflection criteria to size drivetrain components within a geared, upwind wind turbine. Because a full lifetime fatigue load spectrum can only be defined using computationally-expensive simulations in programs such as FAST, a parameterized fatigue loads spectrum that depends on wind conditions, rotor diameter, and turbine design life has been implemented. The parameterized fatigue spectrum is only used in this paper to demonstrate the proposed fatigue analysis approach. This paper details a three-part investigation of the parameterized approach and a comparison of the DriveSE model with and without fatigue analysis on the main shaft system. It compares loads from three turbines of varying size and determines if and when fatigue governs drivetrain sizing compared to extreme load-driven design. It also investigates the model's sensitivity to shaft material parameters. The intent of this paper is to demonstrate how fatigue considerations in addition to extreme loads can be brought into a system engineering optimization.

Nomenclature

A_w	Weibull scale parameter, wind speed probability distribution, m/s
B	Blade number
b	Fatigue component
c	Characteristic chord length of blade at $r = 2/3R$, m
C_L	Lift coefficient of blade at $r = 2/3R$
F	Force, N
f	Frequency, Hz
I_t	Turbulence intensity
L_{rb}	Distance from rotor to upwind main bearing, m
L_{mb}	Length between main bearings, m
k_w	Weibull shape parameter, wind speed probability distribution
M	Moment, Nm
N	Number of loads
p_o	Aerodynamic line load on the blades

*The submitted manuscript has been offered by employees of the Alliance for Sustainable Energy, LLC (Alliance), a contractor of the U.S. Government under Contract No. DE-AC36-08GO28308. Accordingly, the U.S. Government and Alliance retain a nonexclusive royalty-free license to publish or reproduce the published form of this contribution, or allow others to do so, for U.S. Government purposes.

[†]Research Participant, National Wind Technology Center, 15013 Denver West Parkway, Golden, CO, AIAA Student Member.

[‡]Research Engineer, National Wind Technology Center, 15013 Denver West Parkway, Golden, CO

[§]Chief Engineer, National Wind Technology Center, 15013 Denver West Parkway, Golden, CO, AIAA member.

[¶]Senior Engineer, National Wind Technology Center, 15013 Denver West Parkway, Golden, CO.

^{||}Senior Engineer, National Wind Technology Center, 15013 Denver West Parkway, Golden, CO.

R	Rotor radius, m
SUT	Ultimate tensile strength
T_L	Turbine design life, $yr.$
V_{min}	Cut-in wind speed, m/s
V_{max}	Cut-out wind speed, m/s
V_0	Nominal wind speed, m/s
X	Tip speed ratio
W	Resulting wind speed, m/s
$beta$	Scaling variable that takes into account the turbulence intensity
γ	Shaft angle from horizontal, $degree$
ρ_a	Density of air kg/m^3
<i>Subscript</i>	
c	Characteristic load
r	Rotor
$mb1$	Upwind main bearing
$mb2$	Downwind main bearing
<i>Superscript</i>	
x	Coordinate axis x-direction
y	Coordinate axis y-direction
z	Coordinate axis z-direction
st	Stochastic load
dt	Deterministic load

I. Introduction

WIND turbine design software models involve numerous input variables. These variables impact the mass and cost of components throughout the system. Such variables include wind conditions that affect aerodynamic loading, design parameters such as the location and configuration of load-bearing components, and material choices for individual subcomponents of a turbine. As a part of the Systems Engineering effort at the National Wind Technology Center, several sets of analysis models have been created whose primary function is to mimic the design process in place for modern wind turbines to optimize configurations for the lowest cost of energy.

DriveSE is an OpenMDAO-based drivetrain sizing model that considers stress and deflection criteria to size the main shaft, bearings, gearbox, high-speed shaft, generator, bedplate, and other nacelle components of turbines under several configurations. OpenMDAO is an open-source high-performance computing platform for systems analysis and multidisciplinary optimization. This study uses DriveSE and the capability for fatigue analysis is under development and can be implemented for the main shaft and bearings. A full lifetime fatigue load spectrum is typically difficult to define without computationally expensive simulations in programs such as FAST.³ It is also difficult to accurately connect the effects of input changes on stochastic extreme load outputs. For these reasons, simplified parameterized fatigue loads spectra, which depend on wind conditions, rotor diameter, and turbine design life, have been implemented as placeholders for further fatigue analysis. The benefits of this approach are its computational speed and ease of use, but its simplified nature makes it impossible to capture changes in blade design, improvements in controllers, and certain site-specific conditions that are not seen in the model inputs.

This paper details a three-part investigation of the approach and a comparison of the DriveSE model with and without fatigue analysis. It begins by comparing loads from three different turbines of varying size and determining if and when fatigue governs sizing according to the current model. It then looks at the model's sensitivity to the fatigue slope exponent of the main shaft material, a variable that has been found to significantly impact component sizing under fatigue. Finally, this paper will showcase the analysis capabilities of DriveSE that cycles through the properties of known high-strength steel materials and selects the one that produces the lowest assembly mass.

II. DriveSE Approach

A full paper documenting the DriveSE model approach can be found on the Wind-Plant Integrated System Design and Engineering Model (WISDEMTM) website.¹ A short description of the model and its functions is included here for the purpose of identifying how the effects of fatigue are modeled in DriveSE.

1. Extreme Loads Analysis

DriveSE models the main shaft as a hollow high-strength steel shaft that is normally tapered between upwind and downwind bearings for a four-point suspension drivetrain.^{1,2} Shaft length determination depends on a deflection criterion at the location of the main bearings, and shaft diameter design depends on the highest stresses experienced at stress concentration locations, typically at the main bearing locations. Figure 1 shows the force diagram of a main shaft in such a drivetrain.

The input loads for the shaft and bearing model can be taken from a variety of sources, including simulations such as FAST³ in conjunction with the postprocessing tool for loads analysis, MExtremes.⁴ A flowchart illustrating the internal shaft and bearing sizing loops is shown in Appendix B.

Bearings are then sized based on the diameter of the shaft at each bearing location. The type of bearing is a user-input design parameter, and can include compact aligning roller bearings (CARBs), spherical roller bearings (SRBs), single-row tapered roller bearings (TRB1), double-row tapered roller bearings (TRB2), cylindrical roller bearings (CRBs), and single-row deep-groove radial ball bearings (RBs).¹ Bearing mass and dimensional data are defined from the bore diameter, which is the same as the main shaft diameter at each bearing location.

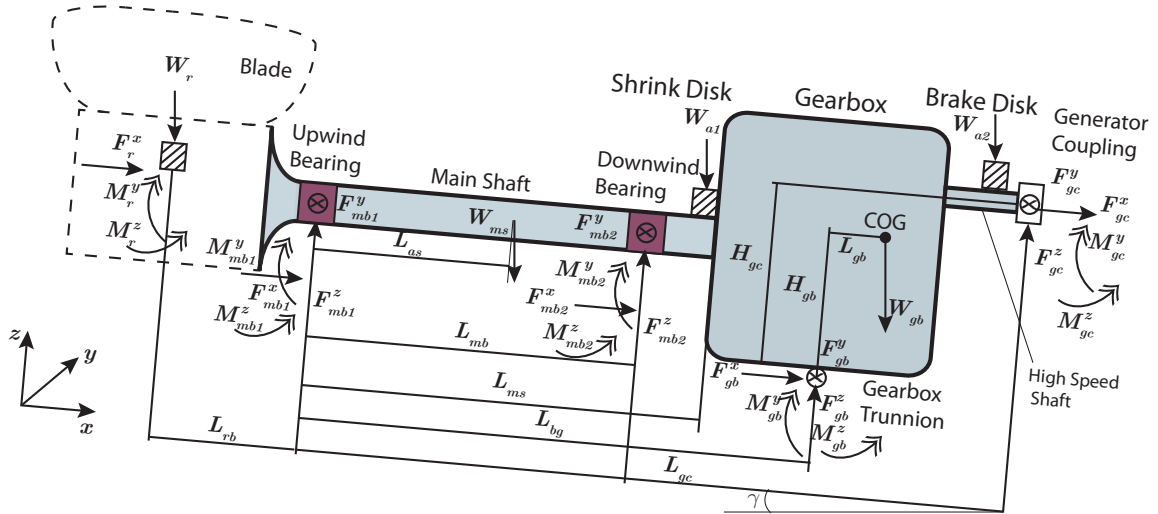


Figure 1: Force diagram of a main shaft in a four-point suspension drivetrain, courtesy of Yi Guo¹

2. Parameterized Fatigue Analysis

Although recognizing that the fatigue loads generated by the parameterized approach are not currently updated or accurate, this study illustrates the application of the fatigue spectrum which is based off of the 1992 Danish design standard DS472⁵ and scaled slightly to match modern technology.¹ This section will briefly touch on the calculations involved in the derivation. See Appendix A for the full mathematical description.

When calculating the maximum number of load cycles experienced by the drivetrain during the life of the turbine, it is assumed that the rated speed of the turbine, its design life, and probability of operation (taken from wind speed probability Weibull parameters and cut-in/cut-out wind speed) can be multiplied to give an approximate lifetime number of shaft rotations, as in Eq. 1.^{1,5}

$$N_f = f_c T_L (\exp(-(V_{min}/A_w)^{k_w}) - \exp(-V_{max}/A_w)^{k_w}) \quad (1)$$

High-cycle fatigue spectra from stochastic wind loading have been found to follow a decreasing logarithmic relationship in the high-cycle region, from large magnitude loads at lower-cycle counts down to lower magnitude loads experienced up to N_f .⁵ The parameterized fatigue spectrum uses this general shape and scales the magnitude of the loads distributions depending on environmental and rotor design variables. Figure 2 shows the general shape of the force and moment ranges as an exceedance plot for a 750-kW machine with a 48-m rotor diameter. All documentation for this derivation can be found in Appendix C. Note that this plot is of the stochastic load ranges, and does not take into account the impact of mean loads such as rotor weight. These load spectra are only used to demonstrate the proposed fatigue analysis approach. They will be compared against measured spectrum in the future.

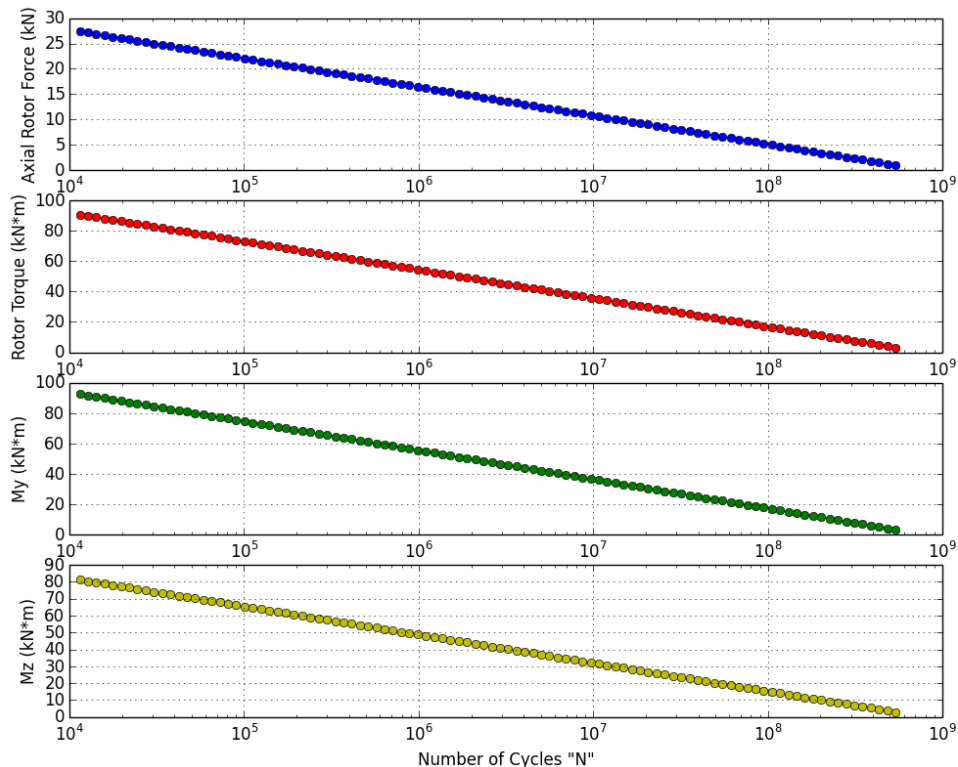


Figure 2: Stochastic wind force and moment cyclic amplitude spectrum defined by the DS472 standard using inputs from a generic 750-kW rotor.

The load ranges described above are accompanied by mean values resulting from component weights, operational torque, and mean axial force. As the design flowchart located in Appendix B shows, the model uses the shaft length and diameter(s) from the extreme loads analysis and increases the shaft diameters if the total damage from high-cycle fatigue results in failure before the design life of the turbine. Damage resulting from each load cycle is assumed to be cumulative, and wake effects from neighboring turbines are not considered in the calculation of aerodynamic rotor load cycles. After the fatigue-driven design of the shaft is complete, the model uses the forces experienced at the bearing locations to calculate fatigue-driven design in the bearing routine. For further detail on the methods used in the DriveSE sizing models, refer to the extensive documentation found in the accompanying drivetrain model report.¹

III. Methods

A. Turbine Comparison

To illustrate the use of parametric fatigue load models in system design calculations, we compare three reference turbines of varying size, define their accompanying extreme loads inputs, and determine the point at which fatigue governs the shaft and bearing sizing of each. Load data are taken from FAST simulations,³ and post-processed in MExtremes.⁴ All Extreme events are cycled as inputs to the DriveSE model, and the

set of design loads that result in the most massive components are taken as the baseline loads inputs for the remainder of the study. The baseline loads for each turbine are included in Table 1.

Table 1: Wind turbine base loads

Loads	750-kW Turbine	1.5-MW Turbine	5-MW Turbine
F_x (kN)	88.305	91.732	254.475
F_y (kN)	2.4435	-77.703	-179.145
F_z (kN)	-183.3	-332.64	-1364.85
M_x (kNm)	434.7	949.59	4942.35
M_y (kNm)	-807.222	1336.223	14053.5
M_z (kNm)	-375.3	-918.405	-5404.05

Because the fatigue model resizes the main shaft diameters up from those of the extreme loads model, a way of quantifying which load set governs the shaft diameter is needed. A multiplier is added to the set of baseline loads and scaled linearly until the point at which the shaft diameters transition from fatigue governance to extreme loads governance. If the extreme loads multiplier at the transition point is greater than 1, then fatigue governs sizing under normal conditions, according to the model. In this way, the multiplier at the transition point is used to gauge which loads set governs shaft sizing and by how much.

1. GRC 750-kW Turbine

The Gearbox Reliability Collaborative (GRC) 750-kW wind turbine is a stall-regulated, three-bladed upwind turbine which resulted from an NREL effort to reveal the causes and loading conditions that cause gearbox failures.¹⁴ Its simple modular configuration and open-source design have been used in several alternative designs as a baseline design and to illustrate a typical drivetrain configuration. Despite the GRC turbine’s three-point suspension design, this study modified the design as four-point suspension for the purpose of analyzing and comparing the fatigue effects on downwind bearings for all three turbine sizes. Further turbine characteristics are included in Table 2.^a

2. WindPACT 1.5-MW Turbine

The Wind Partnership for Advanced Component Technologies (WindPACT) 1.5-MW turbine is the result of an NREL-funded study on how new technologies and larger rotors would affect the cost of energy.¹² The WindPACT study examined several nameplate sizes, however, we focus only on the 1.5-MW nameplate baseline design as it is similar to a turbine that was commonly installed in the United States. The WindPACT 1.5-MW turbine is a three-bladed, upwind, variable-speed, variable-pitch wind turbine design. Details on the WindPACT 1.5-MW turbine are also included in Table 2.

Table 2: Wind turbine specifications

	750-kW	1.5-MW	5-MW
Rotor Diameter (m)	48.2	70	126
Hub Height (m)	55	84	90
Cut-in, Cut-out Wind Speed(m/s)	3,25	4,25	3,25
Gearbox Ratio	81:1	78:1	97:1
Overhang Distance from the hub to the yaw system (m)	2.26	3.3	5
L_{rb} (m) †	1.22	1.535	1.912
Tower Top Diameter (m)	2.2	2.3	3.78

† See Figure 1 for graphical definition. Important moment arm from rotor loads to upwind bearing.

^aGRC was mainly concerned with the input torque to the gearbox, and accordingly ran only the DLCs which may produce a failure event in this assembly: DLC’s 1.2-1.5, 6.1, 6.3, and 7.1 were analyzed and re-run through MExtremes for the purpose of this study.

3. NREL 5-MW Turbine

The NREL 5-MW reference turbine is a conventional utility-scale turbine with a three-bladed, upwind, variable-speed, variable-pitch design. It is loosely based on the REpower 5-MW, Recommendations for Design of Offshore Wind Turbines (RECOFF),⁶ and Dutch Offshore Wind Energy Converter (DOWEC)⁷ designs and the turbine is representative of offshore turbines of a similar nameplate power rating. It is commonly used as a baseline design for wind energy research on diverse topics such as hydrodynamics of floating turbines,⁸ blade design,⁹ and many others. Relevant geometrical and mass properties for the NREL 5-MW reference turbine and its drivetrain are given in Table 2.¹⁰ Loads data were taken from a 2014 NREL study on the effects of tip speed constraints on optimized design.^{11b}

B. Fatigue Exponent Sensitivity

An investigation of the model’s sensitivity to the main shaft fatigue exponent was performed to show the significant impact this variable can have on the design of components in high-cycle fatigue situations, and to determine if the default value is suitable for a general analysis in which the material properties of components are not known.^c Keeping all other inputs equal, we cycled through the exponent range from 1/0.6 to 1/0.12, which encompasses high-strength steels that are commonly used in main shafts.^{1,18,19} The data are processed to find at which loads multipliers fatigue no longer resizes the main shaft, and conclusions can be drawn from the relationship between fatigue exponent and transition point. This yields insight into which set of loads are design drivers at each data point, and with how much confidence.

C. Material Analysis

This portion of the study shows DriveSE’s capabilities for machine design analysis of individual components and assemblies. Recognizing that fatigue exponent is closely coupled with a material’s other strength characteristics, the model calculates component and assembly masses after 38 steel materials are applied to the main shaft model. Variables that define the S-N relationship of the metal reflect real-world materials data taken from two sources.^{18,19} A full input table for this analysis is included in Appendix C. A file with these material properties is run in DriveSE and dimensional results for all affected components are recorded for analysis. For this analysis, all steel densities are assumed to be constant, and the simulation objective is to minimize mass independent of material costs.

IV. Results

A. Turbine Comparison Results

Figure 3 show the results of manipulating the extreme loads multiplier on the shaft/bearing diameters and bearing masses for the 750-kW machine. Each of the turbines exhibit a pattern where upwind diameters are slightly larger in both extreme loads and fatigue analyses. The transition from fatigue to extreme loads is shown to occur at a higher loads multiplier for the upwind bearing, meaning this model predicts that fatigue will govern shaft sizing on the upwind bearing more often than the downwind. The larger difference between bearing masses reflects the fact that this study uses heavier CARB bearings that can support the higher loads for the upwind bearings and lighter SRB bearings for the downwind.

Table 3 shows the loads multiplier at the transition point for each of the three machines. Fatigue analysis resized the upwind diameters of the two larger turbines and nearly had an impact on the upwind diameter of the GRC turbine and the downwind diameter of the 5-MW turbine. These results indicate that the parameterized fatigue spectra for fatigue analysis may approximate loads that are uncharacteristically high for turbines with larger rotor diameters.

^bThis study did not run all design load cases (DLCs) for the turbine, notably omitting DLC 1.4, 6.2, and 6.3 due to lack of yaw controller in simulations. In other turbines where these DLCs were run, they did not contain the baseline loads selected.

^cOther sensitivity tests were performed on wind variables such as International Electrotechnical Commission (IEC) class and wind speeds, but the parameters manipulated the stochastic load ranges as expected and did not produce any striking conclusions.

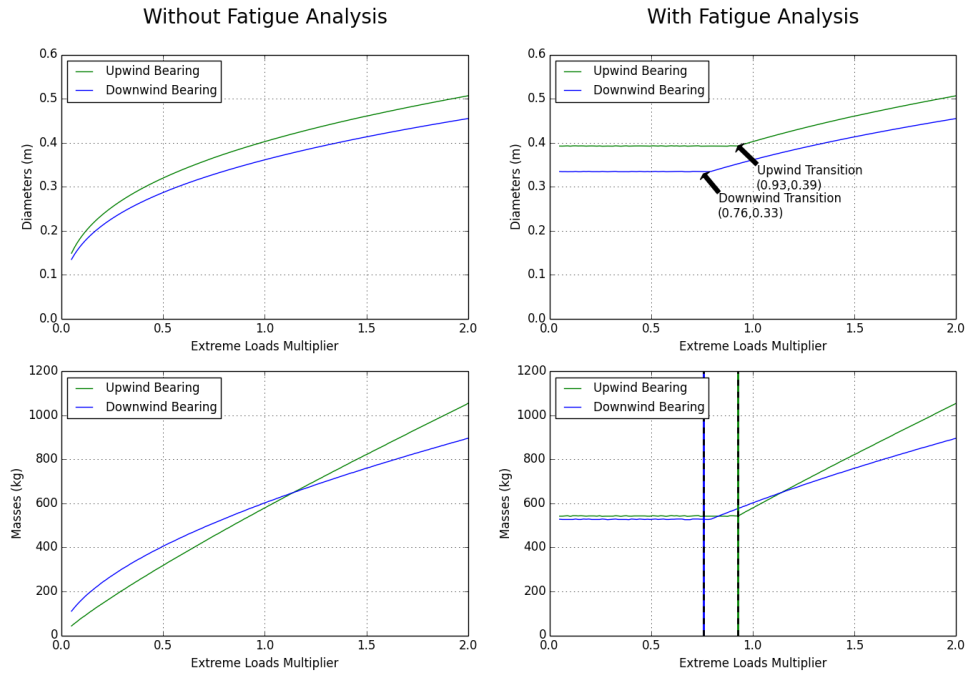


Figure 3: GRC 750-kW bearing diameter and mass results with fatigue-extreme load transition

Table 3: Comparison of extreme loads multipliers at transition point by turbine

	GRC 750-kW Turbine	WindPACT 1.5-MW Turbine	NREL 5-MW Turbine
Upwind Multiplier	0.93	1.31	1.46
Downwind Multiplier	0.76	0.7	0.97

Table 4 compares the shaft dimensions from data sheets to those according to the DriveSE models. We see that in the case of the WindPACT turbine, the fatigue model resizes the shaft to be closer to the expected diameter, but for the 5-MW case, the diameter is too large. This could be due to a variety of reasons, including different material properties for each shaft, the theory that the load ranges do not scale well for the larger machines, or because the dimensions of the 5-MW shaft are only approximations.

Table 4: Comparison of shaft diameters with and without fatigue

	Property	GRC 750-kW Turbine	WindPACT 1.5-MW Turbine	NREL 5-MW Turbine
Actual Dimensions	Upwind Diameter (m)	0.38	0.60	1.00*
	Downwind Diameter (m)	0.33	0.51	0.72*
Design Without Fatigue	Upwind Diameter (m)	0.40	0.48	0.96
	Downwind Diameter (m)	0.36	0.48	0.87
Design With Fatigue	Upwind Diameter (m)	0.40	0.53	1.09
	Downwind Diameter (m)	0.36	0.48	0.87

* In the 5-MW case, approximate diameters were calculated from torsional stiffness and length constraints¹⁰ due to a lack of specified dimensions.

Because the dimensions of the 750-kW shaft are larger than expected regardless of fatigue analysis, one might observe that either the extreme loads from the 750-kW machine are larger than what the turbine would experience, or the dimensions of the shaft in the 750-kW machine are not what they would be for a fully designed and manufactured machine of its size. On the first point, the 750-kW turbine is simulated

as a stall-regulated machine,¹⁴ which would change the aerodynamic rotor loads from its pitch-regulated counterparts. This could be why the extreme loads analysis governs shaft sizes for this machine. This would not, however, invalidate the observation that fatigue dominates sizing for larger turbines, because according to Table 3, the effects of fatigue are significantly more pronounced for the 5-MW turbine than for the 1.5-MW turbine, which are both pitch-regulated machines. On the second point, it is important to note that the 750-kW was created for the purpose of studying gearboxes, and that the optimal size for other components were not thoroughly studied.

The results of this analysis show that the approach that uses FAST loads outputs to DriveSE is relatively accurate with both extreme loads analysis and the additional fatigue option. However, the model does not accurately capture the effects of every input parameter on the shaft assembly dimensions. One important conclusion from this comparison is that the parameterized fatigue spectra, which were originally derived for small-scale stall-regulated machines, may not reflect the fatigue loads coming from the rotors of larger, more modern turbines as accurately as software models require. This shortcoming is especially pronounced if changes to rotor or controller design are made that do not impact the limited fatigue input parameters.

B. Fatigue Exponent Sensitivity Results

Figure 4 shows the effects of manipulating shaft fatigue exponents on the main shaft model for the 5-MW turbine, assuming constant ultimate strengths. From a fatigue exponent of -0.12 to -0.10, the model exhibits a transition from strong effects of fatigue on bearing sizing to no effect. This exemplifies the fact that shaft design under fatigue is highly sensitive to this parameter.

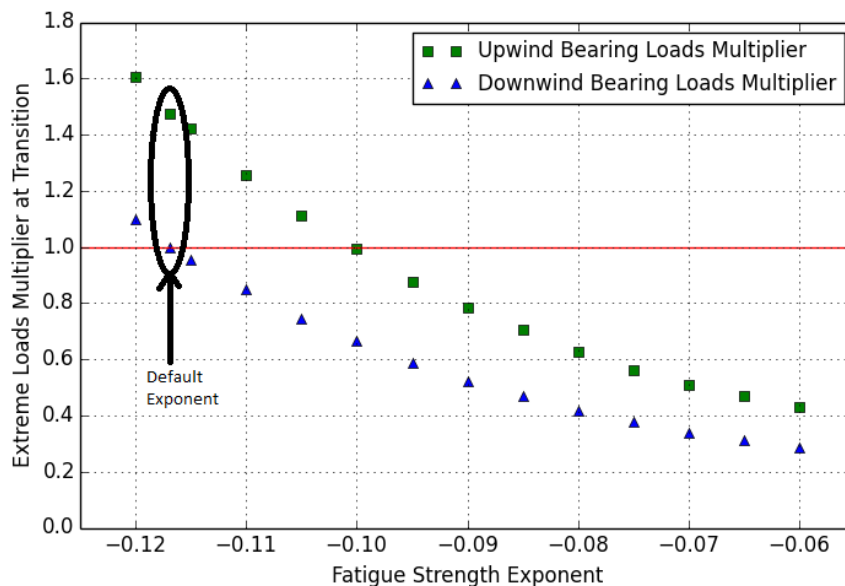


Figure 4: Effects of shaft strength exponent on which loads determine shaft sizing

These results span the range of exponents observed in high-strength steel alloys commonly found in wind turbine main shafts. However, if lower-strength alloys were used in this model, the results would either be massive shafts and bearings that increase the mass and cost of the nacelle, or components that will experience high-cycle fatigue failure within their operational lifetimes. Regardless of the accuracy of the fatigue loads spectrum used in the model, future efforts to model components under fatigue loading must pay close attention to the material properties selected for their components.

As Figure 4 conveys, the model's default exponent of -0.117, the one which was used in the turbine comparison, will often emphasize fatigue effects more than other high-strength steel properties. If mass savings were the only objective, a lower-exponent material should always be selected.

C. Materials Analysis Results

The results of the 5-MW shaft design with all properties from the material table applied to the model are plotted in Figures 6 and 5. A full table with assembly masses, diameters, and nacelle masses from each material simulation is located in Appendix C.

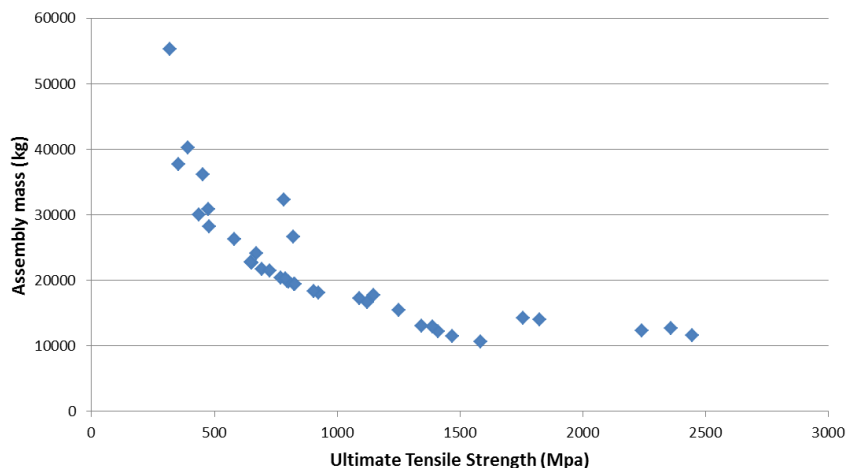


Figure 5: Ultimate tensile strength vs main shaft and bearing assembly mass

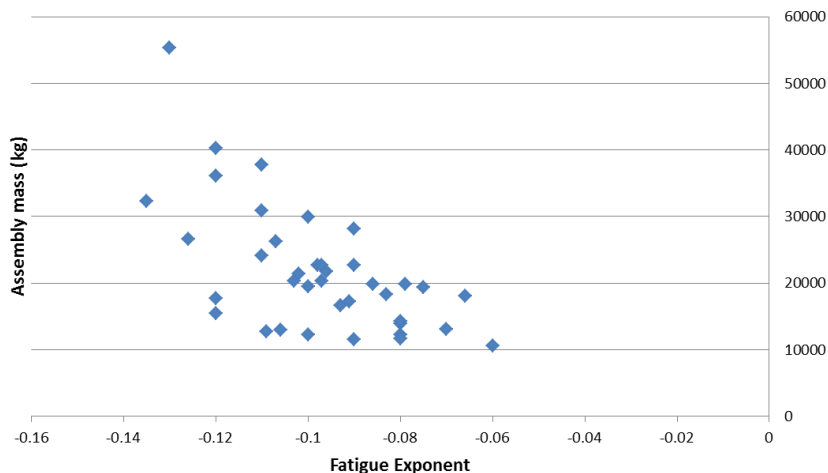


Figure 6: Fatigue exponent vs main shaft and bearing assembly mass

In Figure 5, we see that the strength of the shaft affects the sizing as we might expect. The ultimate tensile strength helps to define both the yield stress criteria on which the main shaft is sized under extreme loads, and the point at which the material fails at $N=1$ cycles on the S-N curve. Because of this strong coupling to both analysis techniques, very little scatter exists in Figure 5.

The relationship between fatigue exponent and assembly mass shown in Figure 6 is still a defined downward trend, but with significantly more “noise” because this variable does not always have an effect on shaft sizing. Even when fatigue does not have an effect on the diameter of the shaft, this relationship would still be present because fatigue exponents of a lower magnitude are normally accompanied with higher strengths.

V. Conclusion

Because of its purely physics-based sizing approach, a comparison between DriveSE outputs and known dimensions demonstrates that the model is relatively accurate for the studied turbines. It illustrates that

the sizing of the main shaft, and consequently the size of the bearings, are very sensitive to the main shaft fatigue exponent. When using the DriveSE fatigue analysis, great care must be taken to ensure accurate material properties are used. For the purposes of general case studies and modeling, the default fatigue exponent of -0.117 and tensile strength of 700 MPa is shown to be a reasonable representation of main shaft materials used in the commercial-scale wind industry. These default parameters have been demonstrated to resize the upwind bearing of a four-point suspension drivetrain more frequently than the downwind bearing because of the higher magnitudes of cyclic loads experienced at this location. The parameterized fatigue loads approach is shown to be a workable means of including the fatigue assessment in a system optimization study. However, much work needs to be done to accurately define the parameterized load spectra for a particular turbine design for the large, pitch-controlled, current generation of wind turbines.

Appendix A: Fatigue Loads Definition

The aerodynamic stochastic loads spectra originate from a Danish Standard published in 1992.⁵ This standard gives an idealized load distribution expressed in terms of wind speed characteristics, International Electrotechnical Commission (IEC) class,¹⁵ the design life of the turbine (generally 20 years), rotor diameter and rated rpm. DS472 is based on the aerodynamic line load on the blades, p_0 [N/m], and is calculated in Eq. (2). The load distribution along a single blade is then represented as a triangular line load with a value of p_0 at the blade tip and 0 at the hub. This value comes into play in subsequent calculations of aerodynamic loading on the rotor:

$$p_o = \frac{1}{2}\rho_a W^2 c_{CL} \quad (2)$$

where the resulting wind speed, W , is found from the following:

$$W^2 = \left(\frac{4\pi}{3} f_r R\right)^2 + V_0^2 \quad (3)$$

To limit the number of inputs needed for the fatigue model, a generalized chord length was calculated from the optimization equation,¹⁷ as shown in Eq. (4). In studies involving an entire turbine, this variable is linked to the WISDEM rotor model, RotorSE.

$$c(r) = \frac{16\pi R}{9BC_L} \frac{1}{X\sqrt{X^2\left(\frac{r}{R}\right)^2 + \frac{4}{9}}} \quad (4)$$

Combining Eqs. (2), (3), and (4) results in a simplified equation for the aerodynamic line load on the blades:

$$p_o = \frac{4}{3}\rho_a \left[\left(\frac{4\pi}{3}\right)^2 + V_0^2 \right] * \left[\frac{\pi * R}{BX\sqrt{X^2 + 1}} \right] \quad (5)$$

To define the total number of load cycles experienced throughout the turbine life, the probability of operation is approximated from the cut-in and cut-out wind speeds and the U_{10} Weibull parameters. This probability is then multiplied by the number of rotor rotations during the design life, if the turbine were operating at rated speed the entire time. Equation (1) in the body of the text defines N_F , the maximum number of loads experienced from a load frequency, f_c . To evaluate pressure from the blades of a turbine, f_c is taken to be $f_{rated} * B$, as recommended by the standard. This effectively defines the total number of possible load cycles as $3 \times N_r$ for a three-bladed turbine and $2 \times N_r$ for a two-bladed turbine.

To define a stochastic cyclic load, a standardized, nondimensional load range $F\Delta^*$ is defined as a representation of all load ranges up to this maximum number of cycles. Under DS472, the probability distribution is defined such that $F\Delta^*$ is the load range that is exceeded N times and is found using the following equation:

$$F\Delta^*(N) = \beta(\log_{10}(N_f) - \log_{10}(N)) + 0.18 \quad (6)$$

This creates a definition of the standard load range distribution that shows a low occurrence of high-magnitude loads and a high occurrence of lower magnitude loads. This nondimensional load distribution is

used to form the shape of the rotor force and moment distribution for fatigue analysis. Figure 2 shows an example of this distribution shape applied to the rotor force and moment distributions on a 750-kW rotor.

The variable β is a scaling variable that takes into account the turbulence intensity, I_T , and the 10-min wind speed shape parameter, A_w . β is calculated in Eq. 7. Assuming no adjustment for neighboring turbines, the value for turbulence intensity is found from the user-input IEC class according to Table 5.¹⁵

$$\beta = 0.11k_\beta(I_T + 0.1)(A_w + 4.4) \quad (7)$$

Table 5: Relationship between IEC class and turbulence intensity factor

IEC Class	I_T
A	0.16
B	0.14
C	0.12

In accordance with DS472, the value of k_β is taken to be 2.5. In addition to scaling the variable β , k_β also appears as an added condition to the standardized loads range found in Eq. 6. The condition suggested by DS 472 is that the value of F_Δ^* must not exceed $2k_\beta$. This effectively truncates the extreme values of the nondimensional loads range at approximately 10^3 to 10^4 load counts, which is the beginning of the high-cycle fatigue region.

With F_Δ^* and p_o defined, the stochastic load ranges from the rotor can be calculated according to the relationships in Eq. 8:

$$\begin{cases} F_x^{st} &= 0.5F_\Delta^*(N)p_oRC_{F_x} \\ M_x^{st} &= 0.45F_\Delta^*(N)p_oR^2C_{M_x} \\ M_y^{st} &= 0.33F_\Delta^*(N)k_r p_o R^2 C_{M_y} \\ M_z^{st} &= 0.33F_\Delta^*(N)k_r p_o R^2 C_{M_z} \end{cases} \quad (8)$$

The amplification factor, k_r , depends on the ratio of rotor resonant frequency (n_r) to the lowest resonant frequency of the associated oscillation form (n_o); for M_y and M_z , $n_o = n_r$, leading to an amplification factor value of 0.8.

The factors C_{F_x} , C_{M_x} , C_{M_y} , and C_{M_z} are adjustments to the original spectra defined by DS472 to account for technology changes since its publication. These factors were determined using available industry data on lifetime fatigue loads, which are unfortunately proprietary in nature.

$$\begin{cases} C_{F_x} &= 0.365 \times \log(D_r) - 1.074 \\ C_{M_x} &= 0.0799 \times \log(D_r) - 0.2577 \\ C_{M_y} &= 0.172 \times \log(D_r) - 0.5943 \\ C_{M_z} &= 0.1659 \times \log(D_r) - 0.5795 \end{cases} \quad (9)$$

An example of the output load ranges is shown in Figure 2 in the body of the text. Note that each of these points represents the *range* of a cyclic load occurring a specified number of times. Because calculations of stress for the purposes of damage equivalent loads require stress amplitudes to be used, the model halves these values in subsequent calculations. This distribution is treated as a histogram of loads experienced across the turbine life. A plot of these distributions, much like those found in Figure 2, is also known as an exceedance plot.

In addition to stochastic alternating loads, several deterministic rotor loads are considered for the purpose of fatigue analysis. For example, rotor weight is applied as a deterministic force in the negative z-direction:

$$F_z^{dt} = -W_r \quad (10)$$

From the definition of the line load p_o , the mean rotor force in the x-direction is found to be:

$$F_x^{dt} = \frac{1}{2}p_oRB \quad (11)$$

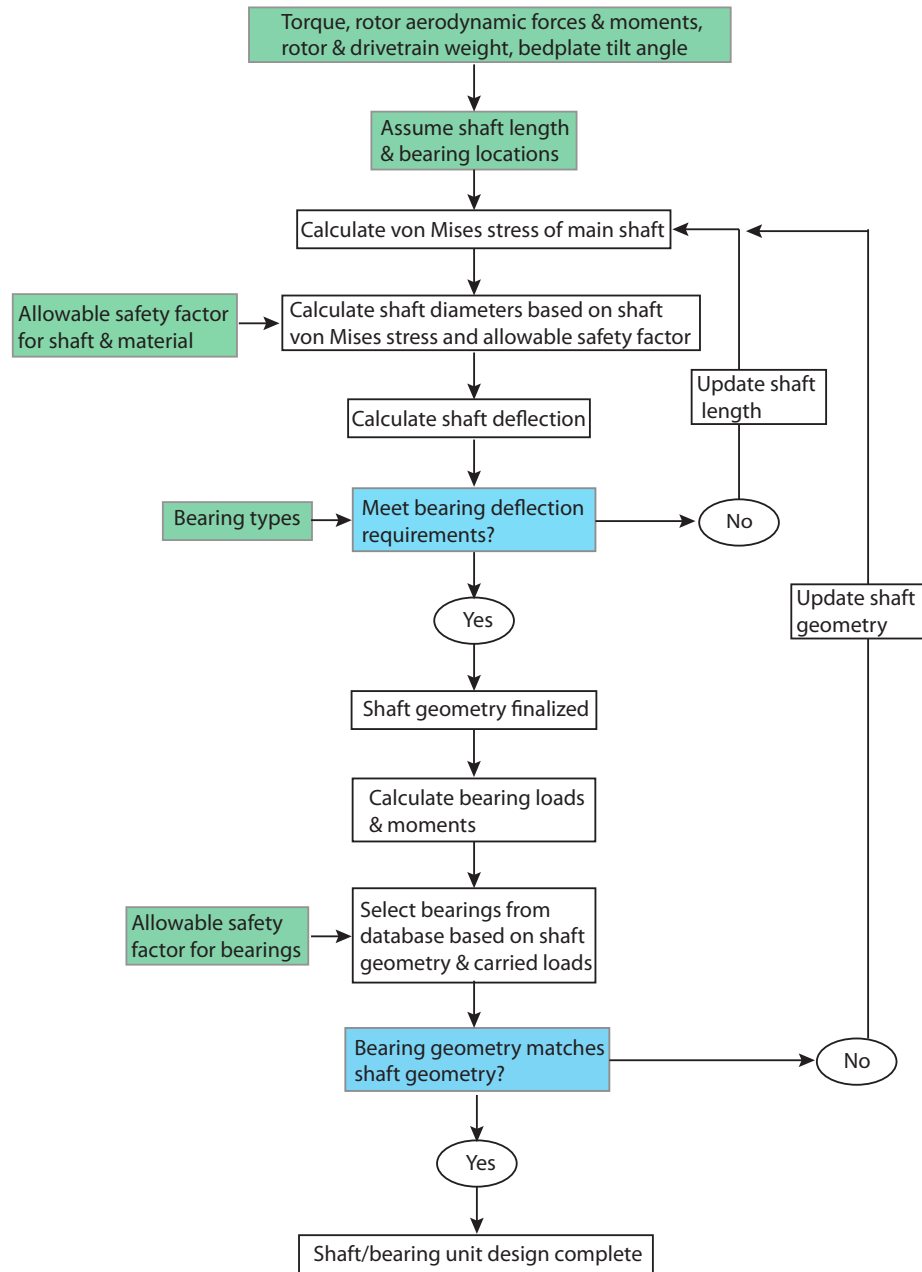
The mean rotor torque during operation is defined as:

$$M_x^{dt} = \frac{P}{\omega \eta_d} \quad (12)$$

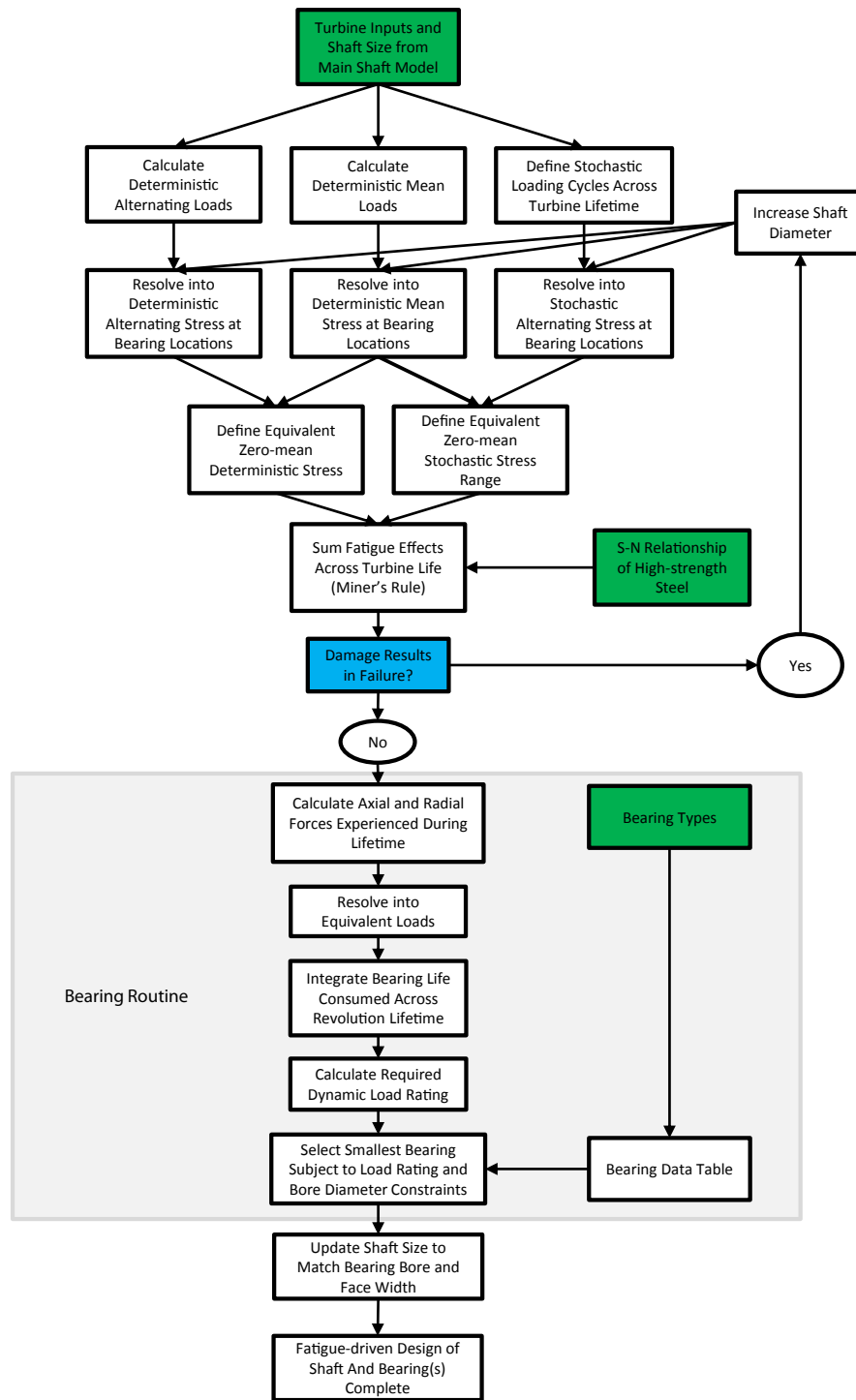
where P is the power rating of the turbine, ω is the rotational velocity of the rotor and drivetrain, and η_d is the drivetrain efficiency.⁵ These mean loads are applied to the fatigue model as mean stress values that are incorporated into the deterministic and stochastic load ranges.

Appendix B: Design Flow for Main Shaft and Bearing System¹

Flowchart for DriveSE shaft and bearing model without fatigue



Flowchart for DriveSE shaft and bearing model with fatigue



Appendix C: Materials and Raw Outputs in Main Shaft Materials Analysis

SAE Steel Grade	Condition	E (Gpa)	Sut (Mpa)	b
1006	As-received	206	318	-0.13
1018	As-received	200	354	-0.11
1020	As-received	186	392	-0.12
1030	As-received	206	454	-0.12
1035	As-received	196	476	-0.11
1045	As-received	216	671	-0.11
1045	QT*	206	1343	-0.07
1045	QT	206	1584	-0.06
1045	QT	206	1825	-0.08
1045	QT	206	2240	-0.1
4142	QT	206	1412	-0.08
4142	QT	206	1757	-0.08
4142	QT	200	2445	-0.08
4340	As-received	192	825	-0.1
4340	QT	200	1467	-0.09
950X	As-rolled	206	438	-0.1
960X	As-rolled	206	480	-0.09
980X	As-rolled	206	652	-0.09
1141	Normalized at 1, 650°F	216	771	-0.097
1141	Reheat, QT	227	925	-0.066
1141	Normalized at 1, 650°F	220	695	-0.096
1141	Reheat, QT	217	802	-0.079
1141	Normalized at 1, 650°F	214	725	-0.102
1141	Reheat, QT	215	797	-0.086
1141	Normalized at 1, 750°F	220	789	-0.103
1038	Normalized at 1, 650°F	201	582	-0.107
1038	Cold size/form	219	652	-0.098
1038	Reheat, QT	219	649	-0.097
1541	Normalized at 1, 650°F	205	783	-0.135
1541	Cold size/form	205	906	-0.083
1050	Normalized at 1, 650°F	211	821	-0.126
1050	Hot forge, cold extrude	203	829	-0.075
1050	Induction through-hardened	203	2360	-0.109
1090	Normalized at 1, 650°F	203	1090	-0.091
1090	Hot form, accelerated cool	203	1388	-0.106
1090	Hot form, QT	217	1147	-0.12
1090	Hot form, austemper	203	1251	-0.12
1090	Hot form, accelerated cool	203	1124	-0.093

* QT= Quenched and Tempered

Acknowledgments

This work was supported by the U.S. Department of Energy under Contract No. DE-AC36-08GO28308 with the National Renewable Energy Laboratory. Funding for the work was provided by the DOE Office of Energy Efficiency and Renewable Energy, Wind and Water Power Technologies Office. The authors would also like to thank Ryan King, who has been available to answer questions and troubleshoot modeling errors from the beginning.

References

- ¹Guo, Y.; Parsons, T.; King, R.; Dykes, K.; Veers, P. "An Analytical Formulation for Sizing and Estimating the Dimensions and Weight of Wind Turbine Drivetrain Components," National Renewable Energy Laboratory, NREL/TP: 5000-63008, 2015.
- ²King, R.; Guo, Y.; Parsons, T.; Dykes, K. (2014). "A Systems Engineering Analysis of 3-point and 4-point Wind Turbine Drivetrain Configurations." National Renewable Energy Laboratory.
- ³Jonkman, J. FAST "An aeroelastic computer-aided engineering tool for horizontal axis wind turbines," Software Package, ver. 7, National Renewable Energy Laboratory, Boulder, CO, URL: <https://nwtc.nrel.gov/FAST7> [cited 31 March 2015].
- ⁴Hayman, G. MExremes, "A MATLAB-based Generator of Extreme-Event Tables," Software Package, Ver. 1.00, National Renewable Energy Laboratory, Boulder, CO, URL: <https://nwtc.nrel.gov/MExremes> [cited 31 March 2015].
- ⁵(1992). DS 472: Loads and Safety of Wind Turbine Construction. 1st ed. Danish Standard Foundation.
- ⁶Frandsen, S.; Tarp-Johansen, N. J.; Norton, E.; Argyriadis, K.; Bulder, B. and Rossis, K. Recommendations for design of offshore wind turbines. Technical Report ENK5-CT-2000-00322, March 2005.
- ⁷H. J. T. Kooijman, C. Lindenburg, D. Winkelaar, and E. L. van der Hooft. "DOWEC 6 MW pre-design". Technical Report DOWEC-F1W2-HJK-01-046/9, Energy Research Center of the Netherlands (ECN), September 2003.
- ⁸Jonkman, J. "Dynamics of offshore floating wind turbines-model development and verification." *Wind Energy*, 12(5):459492, July 2009.
- ⁹Resor, B. "Definition of a 5MW/61.5m wind turbine blade reference model." Sandia Report SAND2013-2569, Sandia National Laboratories, April 2013.
- ¹⁰Jonkman, J.; Butterfield, S.; Musial, W.; Scott, G. "Definition of a 5-MW reference wind turbine for offshore system development." NREL/TP-500-38060, National Renewable Energy Laboratory, February 2009.
- ¹¹Dykes, K.; Platt, A.; Guo, Y.; Ning, N.; King, R.; Parsons, T.; Petch, D.; Veers, P. "Effect of Tip-Speed Constraints on the Optimized Design of a Wind Turbine." National Renewable Energy Laboratory, October 2014
- ¹²Malcolm, D.J.; Hansen, A.C. "WindPACT Turbine Rotor Design Study" NREL/SR-500-32495, June 2000-June 2002
- ¹³Link, H.; LaCava, W.; van Dam, J.; McNiff, B.; Sheng, S.; Wallen, R.; McDade, M.; Lambert, S.; Butterfield, S.; Oyague, F. "Gearbox reliability collaborative project report: findings from phase 1 and phase 2 testing." NREL/TP-5000-51885, 2011.
- ¹⁴Oyague, F. "Gearbox Reliability Collaborative GRC 750 / 48.2 Description and Loading Document (IEC 61400-1 Class IIB)." rev. 3.0 NREL 2010.
- ¹⁵IEC (2005). 61400-1, Design Requirements for wind turbines. International Electrotechnical Commission.
- ¹⁶Dykes, K.; Ning, S. A.; Graf, P.; Scott, G.; Guo, Y.; King, R.; Parsons, T.; Damiani, R.; Fleming, P. "The Wind-Plant Integrated System Design and Engineering Model", National Renewable Energy Laboratory, URL: <https://nwtc.nrel.gov/WISDEM> [cited 30 March 2015].
- ¹⁷Gundtoft, S. "Wind Turbines." University College of Aarhus. 2009.
- ¹⁸Roessle, M.L.; Fatemi, A. "Strain-controlled fatigue properties of steels and some simple approximations." *International Journal of Fatigue* 22 (2000) 495511
- ¹⁹Tartaglia, J. "The Effects of Martensite Content on the Mechanical Properties of Quenched and Tempered 0.2%C-Ni-Cr-Mo Steels." ASM International 1059-9495, June 2009